Electronic Supplementary Material (ESI) for Journal of Materials Chemistry C.
This journal is © The Royal Society of Chemistry 2022

Supporting information

Combing molecular encapsulation and AIE strategy to construct efficient blue TADF polymer for solution-processed multilayer white OLEDs

Xinxin Ban,*[a,b] Tao Zhou,[a] Qingpeng Cao,[a] Kaizhi Zhang,[a] Zhiwei Tong,*[a], Hui Xu,[a] Aiyun Zhu,[a] Wei Jiang*[b]

[a] School of Environmental and Chemical Engineering, Jiangsu Key Laboratory of Function Control Technology for Advanced Materials, Jiangsu Ocean University, Lianyungang, Jiangsu, 222005, China

[b] School of Chemistry and Chemical Engineering, Southeast University, Nanjing, Jiangsu, 211189, China

*Corresponding Authors Email: banxx@jou.edu.cn; zhiweitong575@hotmail.com; jiangw@seu.edu.cn;

General methods

All the reagents used for the synthesis of the compounds were purchased from Energy or aladdin companies and used without further purification. The 1H and 13C NMR spectra were recorded on a BRUKER AMX with tetramethylsilane as internal standards. Elemental analysis was determined by an Elementar Vario EL CHN elemlental analyzer. Matrix-assisted laser desorption ionization time-of-flight (MALDI-TOF) mass spectra were collected on a Bruker Daltonics. The photoluminescence emission spectra were recorded on HORIBA FLUOROMAX-4. The UV-Vis absorption spectra of the compounds were measured by SHIMADZU UV-2450. Thermogravimetric analysis (TGA) and Differential scanning calorimetry (DSC) curves were recorded with a Netzsch simultaneous thermal analyzer (STA) system (STA 409PC) and DSC 2910 modulated calorimeter under a dry nitrogen gas flow at a heating rate of 10 °C min-1. The film surface morphology is performed by the AFM (Seiko Instruments, SPA-400). Cyclic voltammetry (CV) was performed on a CHI750C voltammetric analyzer in a typical three-electrode cell with a platinum plate working electrode, a platinum wire counter electrode and a silver wire reference electrode. All quantum chemical calculations were performed using the Gaussian 09 program package. Geometries in the ground state were optimized using the B3LYP functional with the 6-31G(d) basis set. Low-lying excited energies in singlet and triplet states were obtained using the optimized structures with time dependent density functional theory (TD-DFT) at the same level.

Synthesis and Characterization

Synthesis of (s)-2,3,4,6-tetra(9H-carbazol-9-yl)-5-(4-(2-(4-((4-vinylbenzyl)oxy)phenyl)propan-2-yl)phenoxy)benzonitrile (4CzCN). 4CzFCN (1.0 g, 1.3 mmol), 4-(2-(4-((4-vinylbenzyl)oxy) phenyl)propan-2-yl)phenol (0.5 g, 1.4 mmol), and K_2CO_3 (0.6 g, 4.3 mmol) were dissolved in DMF (40 mL). Stirring for 24 h at RT, the crude yellow product was obtained after removal of the organic solvent. Then, the crude product was further purified by silica gel column chromatography to obtain a yellow powder (0.90 g, 64 % yield). ^{1}H NMR (500 MHz, $CDCl_3$) δ 8.09 (d, *J* = 7.7 Hz, 2H), 7.75 (d, *J* = 7.6 Hz, 2H), 7.67 (d, *J* = 3.9 Hz, 4H), 7.60 (d, *J* = 7.6 Hz, 2H), 7.45 (d, *J* = 8.1 Hz, 2H), 7.40 (dd, *J* = 10.1, 6.4 Hz, 4H), 7.36 – 7.32 (m, 4H), 7.24 (d, *J* = 8.0 Hz, 2H), 7.18 – 6.98 (m, 10H), 6.82 (t, *J* = 7.4 Hz, 2H), 6.74 (d, *J* = 8.9 Hz, 2H), 6.69 (t, *J* = 7.7 Hz, 2H), 6.59 (d, *J* = 8.7 Hz, 2H), 6.27 (d, *J* = 8.8 Hz, 2H), 5.82 (dd, *J* = 27.4, 13.2 Hz, 3H), 5.34 – 5.26 (m, 2H), 5.00 (s, 2H), 1.13 (s, 6H). MS (MALDI-TOF) [m/z]: calcd for $C_{79}H_{55}N_5O_2$, 1105.43; found, 1105.39. Anal. Calcd. for $C_{79}H_{55}N_5O_2$: C, 85.77; H, 5.01; N, 6.33. Found: C, 85.75; H, 5.01; N, 6.32.

Synthesis of (2S,3R,4R,6S)-2,3,4,6-tetrakis(4-(2-(9H-carbazol-9-yl)ethoxy)-9H-carbazol-9-yl)-5-fluorobenzonitrile (Cz4CzFCN). 4-(2-(9H-carbazol-9-yl)ethoxy)-9H-carbazole (4 g, 9.2 mmol) and sodium hydride (0.08 g, 3.3 mmol) was added to the anhydrous THF (50 mL) solution. After stirring vigorously for 30 minutes under a nitrogen atmosphere at room temperature, 2,3,4,5,6-pentafluorobenzonitrile (0.6 g, 3.3 mmol) was added. The mixture was stirred at room temperature for 24 hours. After the reaction was finished, it was poured into distilled water (30 mL) to precipitate a yellow solid. The yellow solid was filtered, dried, and purified by silica gel column chromatography to obtain a bright yellow powder (2.50 g, 54 % yield). ^{1}H NMR (500 MHz, $CDCl_3$) δ 8.40 (d, *J* = 7.3 Hz, 1H), 8.18 – 8.02 (m, 8H), 7.96 (s, 2H), 7.64 – 7.49 (m, 4H), 7.45-7.31 (m, 15H), 7.28 (d, *J* = 8.2 Hz, 2H), 7.26 – 7.11 (m, 12H), 7.06 (dd, *J* = 17.3, 8.4 Hz, 6H), 6.91 (dd, *J* = 18.9, 13.4 Hz, 2H), 6.79 (d, *J* = 7.8 Hz, 2H), 6.70 (s, 2H), 6.62 (d, *J* = 7.7 Hz, 1H), 6.43 (s, 2H), 6.14 (d, *J* = 8.2 Hz, 1H), 4.34 (t, *J* = 7.0 Hz, 2H), 4.29 – 4.09 (m, 8H), 3.90 (s, 4H), 3.64 (s, 2H), 2.02 – 1.91 (m, 4H), 1.88-1.78 (m, 4H), 1.76-1.62 (m, 8H), 1.53 (d, *J* = 5.3 Hz, 4H), 1.41 (d, *J* = 35.2 Hz, 8H), 1.30-1.20 (m, 4H). MS (MALDI-TOF) [m/z]: calcd for $C_{127}H_{108}FN_9O_4$, 1841.85; found, 1841.80. Anal. Calcd. for $C_{127}H_{108}FN_9O_4$: C, 82.75; H, 5.91; N, 6.84. Found: C, 82.75; H, 5.90; N, 6.84.

Synthesis of (2S,3R,4R,6S)-2,3,4,6-tetrakis(4-(2-(9H-carbazol-9-yl)ethoxy)-9H-carbazol-9-yl)-5-(4-(2-(4-((4-vinylbenzyl)oxy)phenyl)propan-2-yl)phenoxy)benzonitrile (Cz4CzCN). Cz4CzFCN (1.0 g, 0.6 mmol), 4-(2-(4-((4-vinylbenzyl)oxy) phenyl)propan-2-yl)phenol (0.3 g, 0.8 mmol), and K_2CO_3 (0.3 g, 2.2 mmol) were dissolved in DMF (30 mL). Stirring for 24 h at RT, the crude yellow product was obtained after removal of the organic solvent. Then, the crude product was further purified by silica gel column chromatography to obtain a yellow powder (0.75 g, 70 % yield). ^{1}H NMR (500 MHz, $CDCl_3$) δ 8.26 (d, *J* = 7.3 Hz, 1H), 8.11 – 8.02 (m, 8H), 7.95 (d, *J* = 7.9 Hz, 2H), 7.79 (d, *J* = 8.3 Hz, 2H), 7.60 – 7.50 (m, 4H), 7.47-7.33 (m, 16H), 7.33 – 7.25 (m, 8H), 7.19 (dt, *J* = 14.4, 7.3 Hz, 10H), 7.11-6.85 (m, 9H), 6.72 (dd, *J* = 15.7, 7.5 Hz, 4H), 6.66 (d, *J* = 8.1 Hz, 2H), 6.55 (d, *J* = 8.3 Hz, 2H), 6.15 (dd, *J* = 16.6, 8.0 Hz, 3H), 5.79 – 5.68 (m, 3H), 5.23 (d, *J* = 10.9 Hz, 1H), 4.88 (s, 2H), 4.33 (t, *J* = 7.1 Hz, 2H), 4.24 (dd, *J* = 16.3, 8.5 Hz, 4H), 4.16 (t, *J* = 6.9 Hz, 4H), 3.96-3.90 (m, 2H), 3.89-3.79 (m, 2H), 3.69 (t, *J* = 7.0 Hz, 2H), 1.99-190 (m, 4H), 1.88 – 1.79 (m, 4H), 1.78 – 1.62 (m, 8H), 1.46-1.33 (m, 8H), 1.32 – 1.21 (m, 8H), 1.06 (s, 6H). MS (MALDI-TOF) [m/z]: calcd for $C_{151}H_{131}N_9O_6$, 2166.02; found, 2166.01. Anal. Calcd. for $C_{151}H_{131}N_9O_6$: C, 83.66; H, 6.09; N, 5.82. Found: C, 83.64; H, 6.09; N, 5.83.

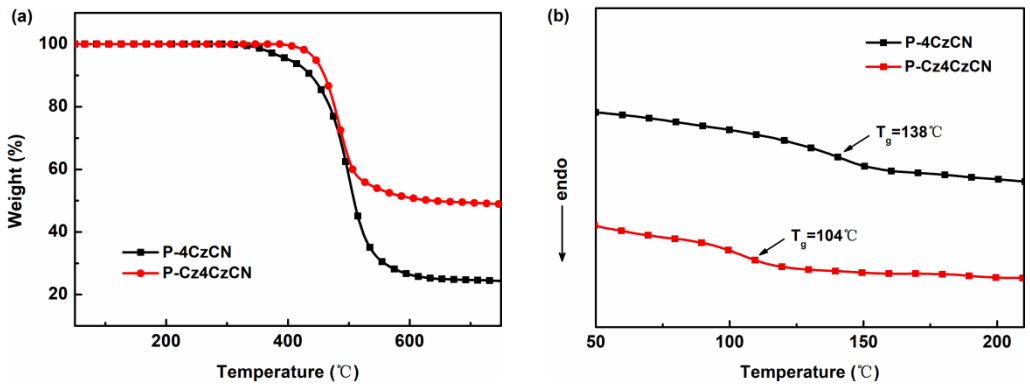

Figure S1. TGA (a) and DSC (b) curves of P-4CzCN and P-Cz4CzCN recorded at a heating rate of 10 °C min^{-1}.

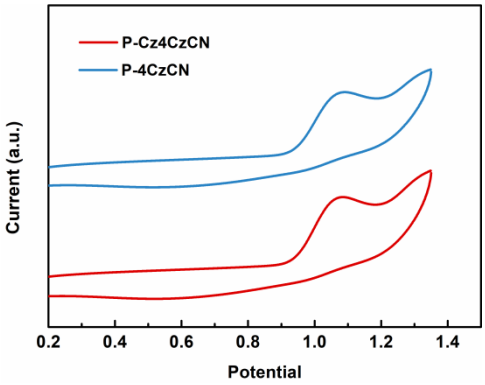

Figure S2. Cyclic voltammetry (CV) curves of P-4CzCN and P-Cz4CzCN measured at room temperature in CH_2Cl_2.

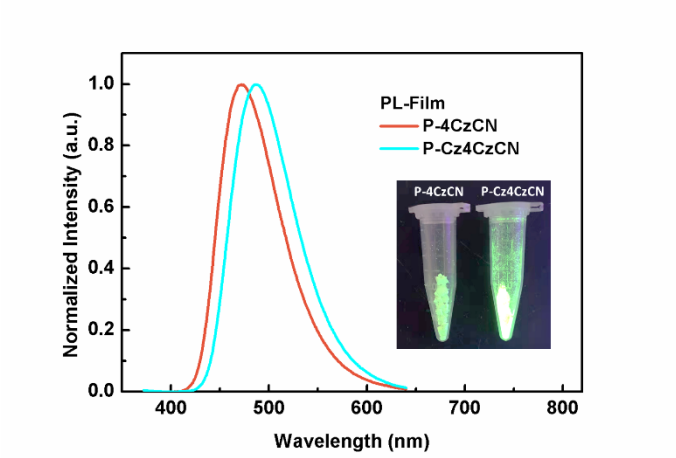

Figure S3. The PL spectra of P-4CzCN and P-Cz4CzCN films.

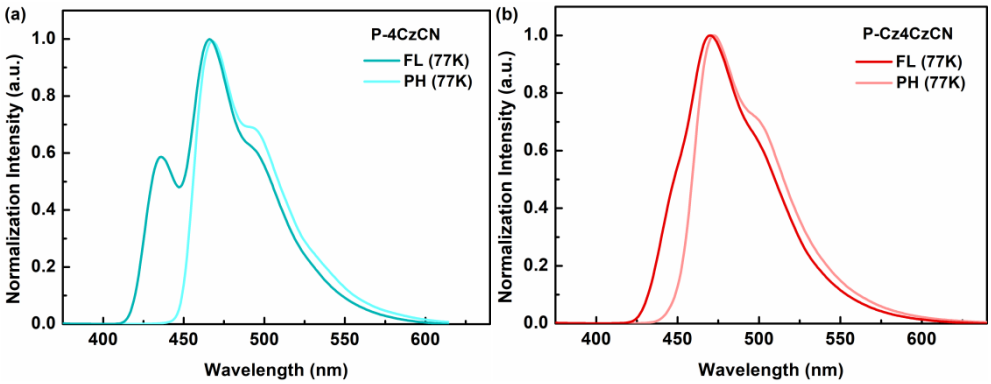

Figure S4. Fluorescence and phosphorescence spectra (measured at 77K) in toluene solution of P-4CzCN and P-Cz4CzCN.

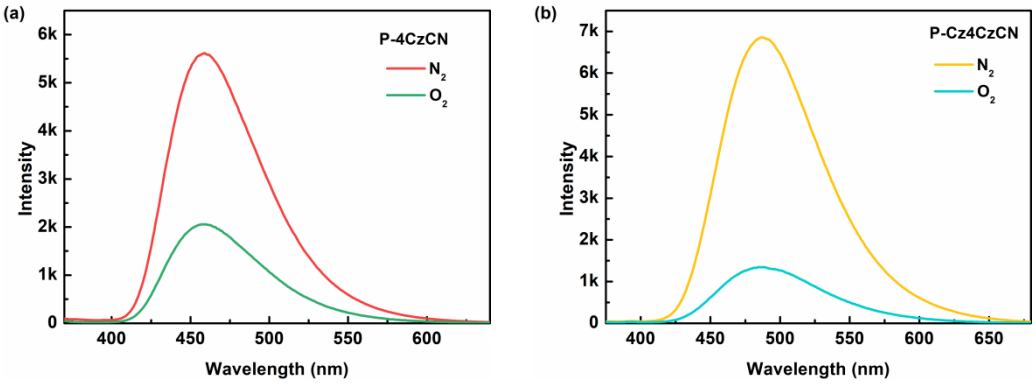

Figure S5. Transient photoluminescence decay curves of P-4CzCN and P-Cz4CzCN in O_2/N_2.

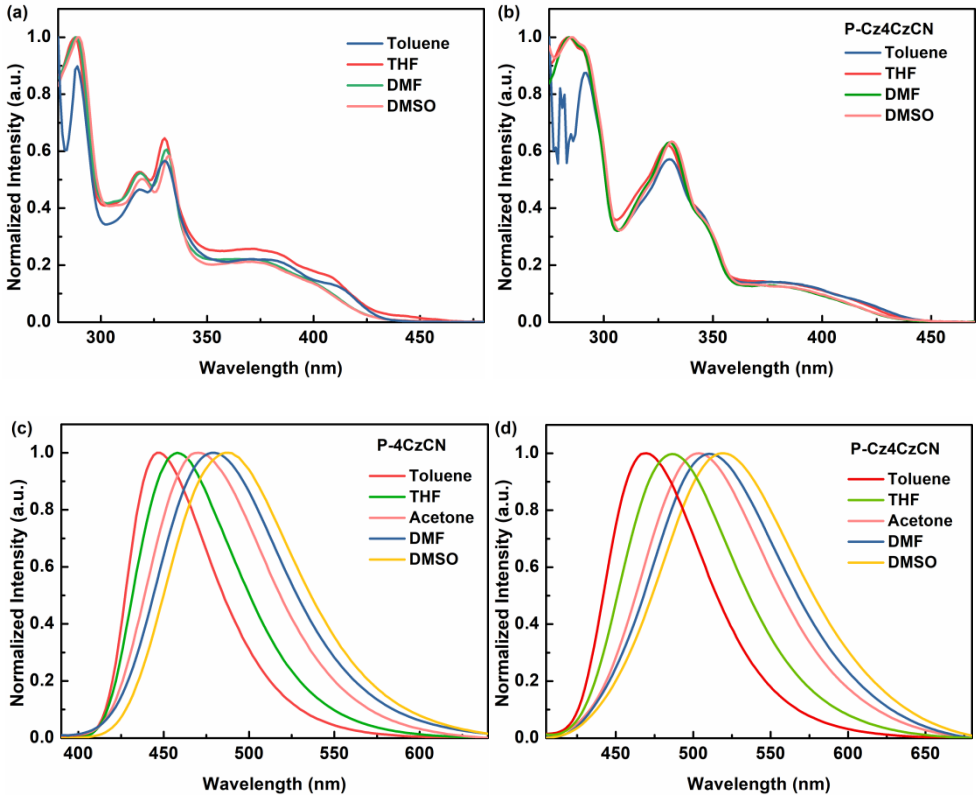

Figure S6. UV and PL spectra of P-4CzCN and P-Cz4CzCN in different solvents.

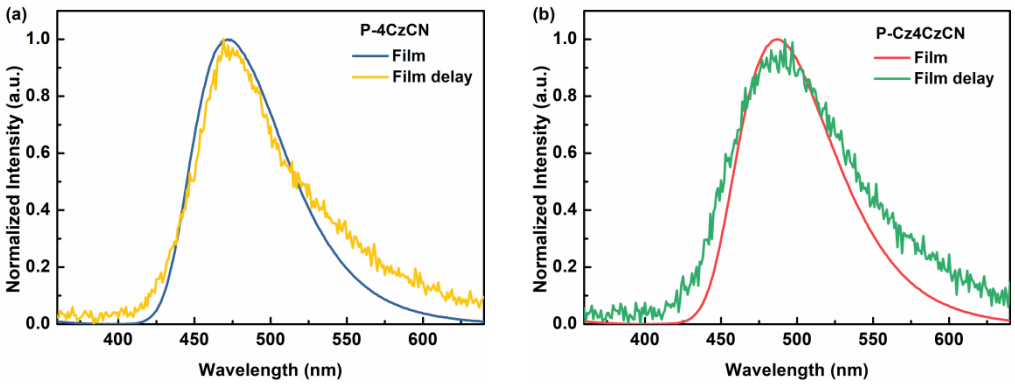

Figure S7. Fluorescence and delay Fluorescence spectra of P-4CzCN and P-Cz4CzCN at room temperature.

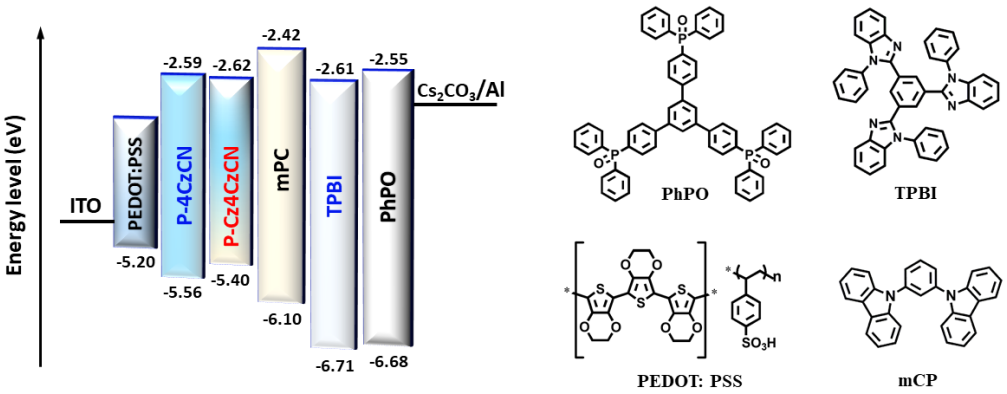

Figure S8. Schematic diagram of the device with the energy levels and molecular structures of the organic compounds.

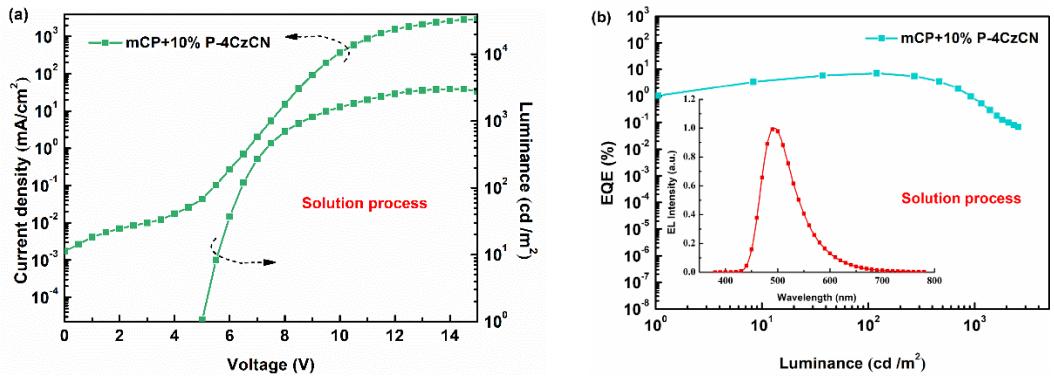

Figure S9. (a) Current density−voltage−luminance (J−V−L) curves; (b) External quantum efficiency (EQE) versus luminance; Inset: the EL spectra for Mcp+10 % P-4CzCN based solution-processed OLEDs.

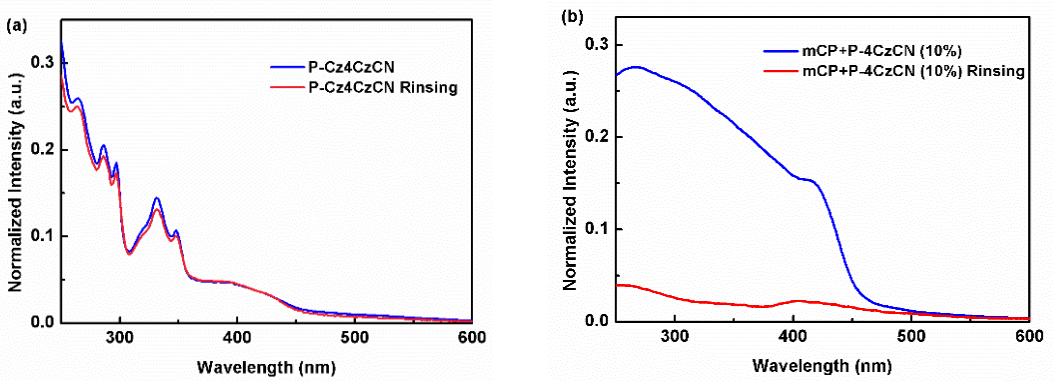

Figure S10. UV-vis spectra of the films before and after post-rinsing process. (a) P-Cz4CzCN, and (b) mCP+10wt%P-4CzCN.

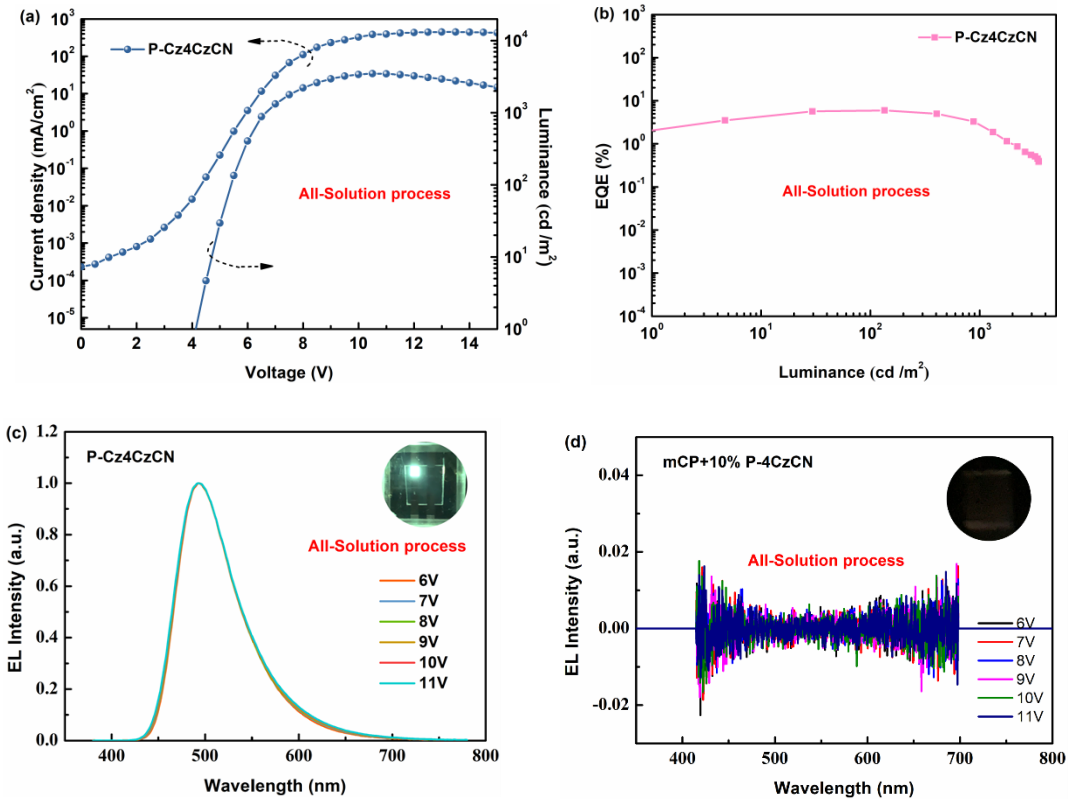

Figure S11. (a) Current density−voltage−luminance (J−V−L) curves; (b) External quantum efficiency (EQE) versus luminance; EL spectra for P-Cz4CzCN (c) and mCP+10 % P-4CzCN (d) based fully-solution-processed OLEDs; Inset: the photo of the device.

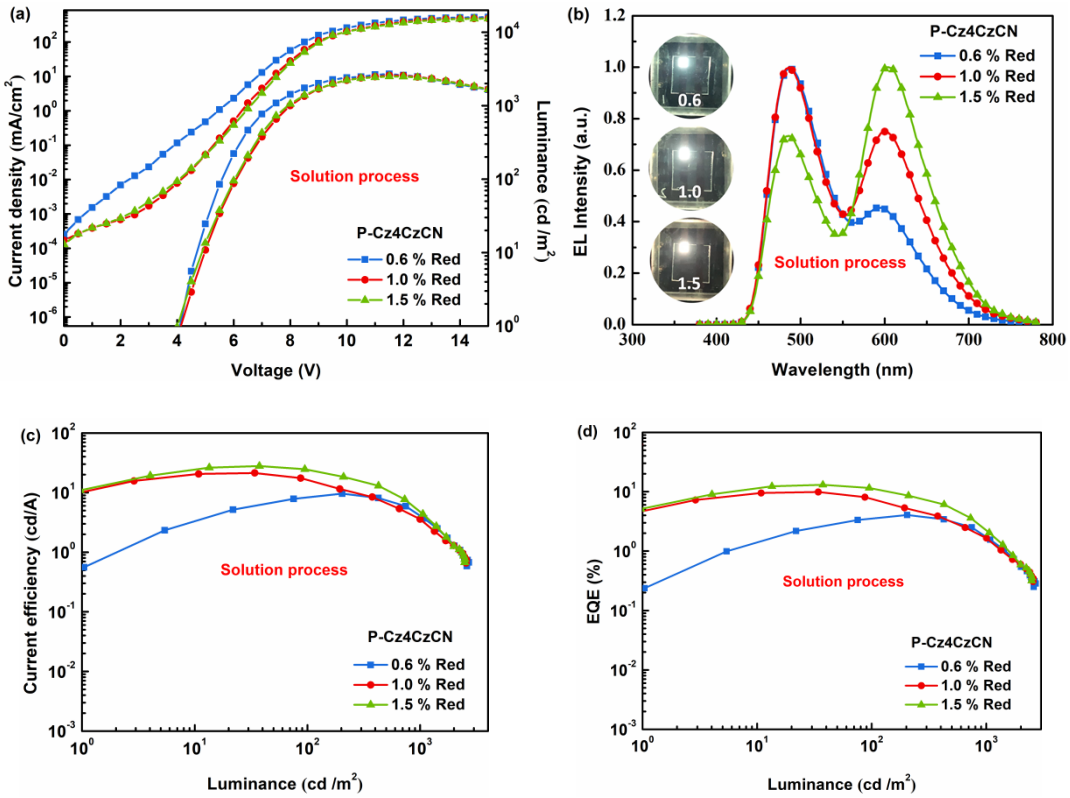

Figure S12. (a) Current density−voltage−luminance (J−V−L) curves; (b) EL spectra with different dopant concentration; (c) External quantum efficiency (EQE) versus luminance; (d) Current efficiency and power efficiency versus luminance for solution-processed white OLEDs with vacuum-deposited TPBI. Inset: the photo of the white emission device.

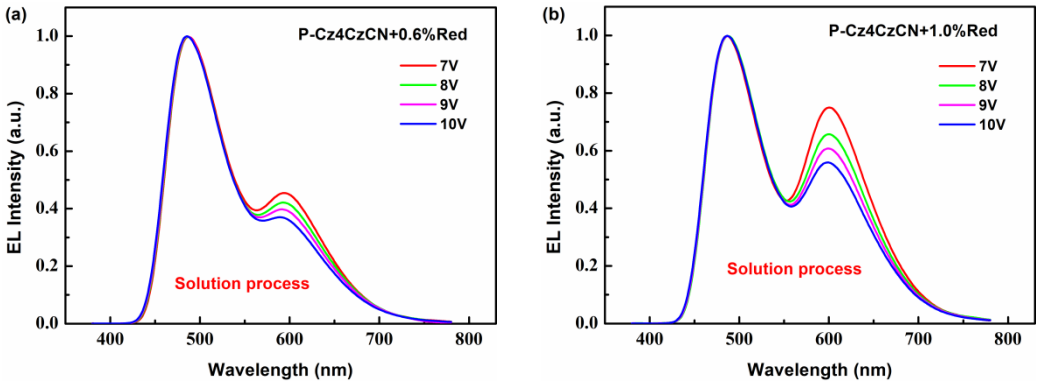

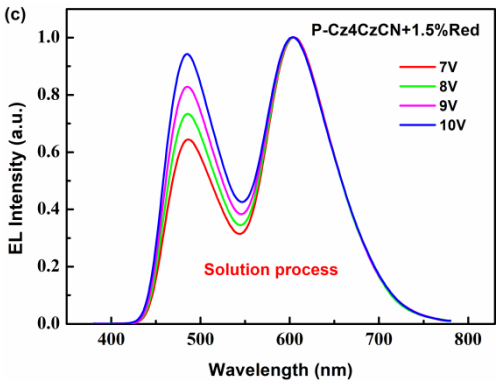

Figure S13. The electro-luminance spectra of the solution-processed white OLEDs based on vacuum deposited TPBI, (a) P-Cz4CzCN+0.6% $Ir(MDQ)_2(acac)$; (b) P-Cz4CzCN+1.0% $Ir(MDQ)_2(acac)$; (c) P-Cz4CzCN+1.5% $Ir(MDQ)_2(acac)$.

(a)

```
Excitation energies and oscillator strengths:

Excited State   1:      Triplet-A     2.5916 eV  478.40 nm  f=0.0000  <S**2>=2.000
    276 -> 300       -0.12155
    280 -> 300        0.10213
    297 -> 300       -0.12398
    298 -> 300        0.21058
    299 -> 300        0.61714
This state for optimization and/or second-order correction.
Total Energy, E(TD-HF/TD-KS) =  -3547.53173690
Copying the excited state density for this state as the 1-particle RhoCI density.

Excited State   2:      Triplet-A     2.7029 eV  458.71 nm  f=0.0000  <S**2>=2.000
    280 -> 300        0.10404
    281 -> 300       -0.11617
    292 -> 300        0.14484
    297 -> 300       -0.19253
    298 -> 300        0.50990
    299 -> 300       -0.30781
    299 -> 301        0.12582

Excited State   3:      Singlet-A     2.7325 eV  453.73 nm  f=0.0633  <S**2>=0.000
    299 -> 300        0.69189

Excited State   4:      Singlet-A     2.9127 eV  425.67 nm  f=0.0045  <S**2>=0.000
    295 -> 300       -0.20312
    297 -> 300       -0.25757
    298 -> 300        0.60995
SavETr:  write IOETrn=   770 NScale= 10 NData=  16 NLR=1 NState=    4 LETran=     82.

 ********************************************************************
```

T1

P-4CzCN

S1

(b)

```
Excited State   1:      Triplet-A     2.5491 eV  486.39 nm  f=0.0000  <S**2>=2.000
    574 -> 584        0.10125
    576 -> 584        0.11372
    580 -> 584       -0.27827
    583 -> 584        0.59117
This state for optimization and/or second-order correction.
Total Energy, E(TD-HF/TD-KS) =  -6856.99675332
Copying the excited state density for this state as the 1-particle RhoCI density.

Excited State   2:      Triplet-A     2.6292 eV  471.57 nm  f=0.0000  <S**2>=2.000
    552 -> 584       -0.11444
    567 -> 584       -0.12003
    574 -> 584       -0.16038
    575 -> 584        0.11745
    576 -> 584       -0.18088
    580 -> 584        0.49472
    583 -> 584        0.33582
    583 -> 585       -0.10971

Excited State   3:      Singlet-A     2.6419 eV  469.29 nm  f=0.0503  <S**2>=0.000
    583 -> 584        0.69055

Excited State   4:      Singlet-A     2.7593 eV  449.33 nm  f=0.0081  <S**2>=0.000
    577 -> 584        0.24770
    580 -> 584        0.64827
SavETr:  write IOETrn=   770 NScale= 10 NData=  16 NLR=1 NState=    4 LETran=     82.

 ********************************************************************

          Population analysis using the SCF density.
```

T1

P-Cz4CzCN

S1

Figure S14. Illustration of S_1 and T_1 raw data of P-4CzCN (a) and P-Cz4CzCN (b) optimized by TD-DFTF method.

Table S1. Photophysical properties of the non-doped films of P-4CzCN and P-Cz4CZCN.

Samples	PLQY [%]	A_1	A_2	τ_1 [ns]	τ_2[ns]	R_{PF}	R_{DF}	Φ_{PF}	Φ_{DF}
P-4CzCN	0.37	15272.89	102.808	15	1500	0.60	0.40	0.222	0.148
P-Cz4CzCN	0.65	11163.48	155.31	25	1900	0.49	0.51	0.318	0.332

A_1/A_2 is the pre-exponential for lifetime τ_1/τ_2. R_{PF} and R_{DF} are individual component ratio for prompt and delayed fluorescence. ($R_{PF} = \tau_1A_1/(\tau_1A_1 + \tau_2A_2)$, $R_{DF} = \tau_2A_2/(\tau_1A_1 + \tau_2A_2)$; $\Phi_{PF} = \Phi_{PL} R_{PF}$, $\Phi_{DF} = \Phi_{PL} R_{DF}$).

Table S2. EQE values of doped and undoped TADF OLED based on polymers in recent years.

EML	Non-doped TADF OLED	EQE_{max} (%)	Ref
P-Cz4CzCN	√	11.5	this work
PTZ-DBTO2	√	3.0	1
PDT-2	√	5.3	2
P6/P9	√	7.0	3
PDCDC	√	9.0	4
LEP	√	10.0	5
TMTPA-DCB	√	15.3	6
TMTPA-DCB: 10% mCP	×	24.0	6
PCzBPCl-10: CBP	×	22.0	7
PCPTCN-1/4: 50% mCP	×	21.1	8
PTZ-DBTO2: CBP	×	19.4	1
mCP:DMAC-DP-Cz:PCzDP-10	×	16.1	9
P(DMTRZ-Cp): 25% mCP	×	15.4	10
A-SM-25 %	×	12.9	11

Reference

1. Nobuyasu, R. S.; Ren, Z.; Griffiths, G. C.; Batsanov, A. S.; Data, P.; Yan, S.; Monkman, A. P.; Bryce, M. R.; Dias, F. B., Rational Design of TADF Polymers Using a Donor-Acceptor Monomer with Enhanced TADF Efficiency Induced by the Energy Alignment of Charge Transfer and Local Triplet Excited States. *Advanced Optical Materials* **2016,** *4* (4), 597-607.
2. Li, C.; Ren, Z.; Sun, X.; Li, H.; Yan, S., Deep-Blue Thermally Activated Delayed Fluorescence Polymers for Nondoped Solution-Processed Organic Light-Emitting Diodes. *Macromolecules* **2019,** *52* (6), 2296-2303.

3. Zhou, X.; Huang, M.; Zeng, X.; Chen, T.; Xie, G.; Yin, X.; Yang, C., Combining the qualities of carbazole and tetraphenyl silane in a desirable main chain for thermally activated delayed fluorescence polymers. *Polymer Chemistry* **2019,** *10* (30), 4201-4208.
4. Li, C.; Harrison, A. K.; Liu, Y.; Zhao, Z.; Dias, F. B.; Zeng, C.; Yan, S.; Bryce, M. R.; Ren, Z., TADF dendronized polymer with vibrationally enhanced direct spin-flip between charge-transfer states for efficient non-doped solution-processed OLEDs. *Chemical Engineering Journal* **2022,** *435*, 134924.
5. Nikolaenko, A. E.; Cass, M.; Bourcet, F.; Mohamad, D.; Roberts, M., Thermally Activated Delayed Fluorescence in Polymers: A New Route toward Highly Efficient Solution Processable OLEDs. *Adv Mater* **2015,** *27* (44), 7236-40.
6. Ding, J.; Rao, J.; Yang, L.; Li, X.; Wang, L., Sterically-locked Donor-Acceptor Conjugated Polymers Showing Efficient Thermally Activated Delayed Fluorescence. *Angewandte Chemie* **2021,** *133*, 9721-9727.
7. Liu, Y.; Hua, L.; Yan, S.; Ren, Z., Halogenated π-conjugated polymeric emitters with thermally activated delayed fluorescence for highly efficient polymer light emitting diodes. *Nano Energy* **2020,** *73*, 104800.
8. Long, Y.; Chen, X.; Wu, H.; Zhou, Z.; Sriram Babu, S.; Wu, M.; Zhao, J.; P. Aldred, M.; Liu, S.; Chen, X.; Chi, Z.; Xu, J.; Zhang, Y., Rigid Polyimides with Thermally Activated Delayed Fluorescence for Polymer Light-Emitting Diodes with High External Quantum Efficiency up to 21%. *Angewandte Chemie* **2021,** *60* (13), 7220-7226.
9. Xie, G.; Luo, J.; Huang, M.; Chen, T.; Wu, K.; Gong, S.; Yang, C., Inheriting the Characteristics of TADF Small Molecule by Side-Chain Engineering Strategy to Enable Bluish-Green Polymers with High PLQYs up to 74% and External Quantum Efficiency over 16% in Light-Emitting Diodes. *Adv Mater* **2017,** *29* (11), 1604223.
10. Kim, H. J.; Lee, C.; Godumala, M.; Choi, S.; Park, S. Y.; Cho, M. J.; Park, S.; Choi, D. H., Solution-Processed Thermally Activated Delayed Fluorescence Organic Light-Emitting Diodes Using New Polymeric Emitter Containing Non-conjugated Cyclohexane Units. *Polymer Chemistry* **2018,** *9*, 1318-1326.
11. Philipps, K.; Ie, Y.; van der Zee, B.; Png, R. Q.; Ho, P. K. H.; Chua, L. L.; Del Pino Rosendo, E.; Ramanan, C.; Wetzelaer, G. A. H.; Blom, P. W. M.; Michels, J. J., Role of Linker Functionality in Polymers Exhibiting Main-Chain Thermally Activated Delayed Fluorescence. *Adv Sci (Weinh)* **2022,** *9* (19), 2200056.